GMRT antenna power pattern in L band

Data from 27-28 December 2000

Nimisha G. Kantharia & A. Pramesh Rao

July 20, 2001

1 Aims

1. To study the shape of the GMRT antenna primary beam - both the elevation and azimuth beams and obtain the half power beam width.
2. To obtain the best polynomial fit to the GMRT antenna primary beam shape required for primary beam response correction in the final analysis using the task PBCOR in AIPS.
3. To study the variation in the pointing offsets with elevation.
4. To study the effect of the FPS position on the elevation beam shape.

2 Introduction

The L band feed consists of a corrugated horn designed and made by the Raman Research Institute. This type of feed has a high aperture efficiency and low cross-polarization levels. The feed receives two linear polarizations which are then further processed. The L band is the only band at GMRT where the two orthogonal linear polarizations are processed and available to the astronomer. As with the rest of the GMRT bands, this feed is also a prime focus feed, positioned at the focus of the parabolic dish and mounted on a turret. The front-end electronics are also mounted on the turret. The flare angle of the corrugated horn is 120°. The feed illuminates the 45-m mesh reflector which has a radially varying mesh size. The inner 1/3rd has a mesh size of 10mm, the middle 1/3rd of 15mm and the outer 1/3rd of 20mm. The wide-band feed has a VSWR < 2 for a bandwidth of 580 MHz - ranging from 1000 MHz to 1580 MHz. This band is divided into 4 sub-bands, each of bandwidth 140 MHz centred on 1060, 1170, 1280 and 1390 MHz. A bypass mode which allows the usage of the entire 580 MHz bandwidth also exists. For our experiment, we used the 1060 MHz and 1280 MHz sub-bands.

The entire experiment was divided into four parts to study four aspects related to the L band beam. The 130 MHz polarization channel was used. The first part concerned the study of the beamshape in both the altitude and azimuth directions and to obtain the half power beamwidth. For this we obtained a one-dimensional cut in elevation and azimuth by observing a grid of points about a strong point source. While the azimuth beam is fairly symmetric, the elevation beam was found to be skewed. The second part was to use this data and find the best polynomial fit to the beamshape. This is required for correcting the GMRT data for the primary beam gain variation. An eight-order polynomial fit was found to fit the azimuth beam well and the results are presented here. In the third part to study the variation in elevation pointing offsets with source elevation, we tracked a strong point source through a run and noted down the offsets. The offsets do not vary significantly, but they do show a systematic variation of $\leq 4'$. Lastly, to obtain an optimum position for the FPS, we wanted to do the fourth part of the experiment by rotating the feed turret to obtain a more-symmetric elevation beam. The data and discussion can be found in another report.

3 On the Observational Data

For the first and second part of the experiment, we observed a one-dimensional grid of points in elevation and azimuth centred on a strong point source (e.g 3C48) as shown in Fig 1. All the antennas except a couple were made to observe the grid points. The remaining two antennas were used as reference and moved to another sub-array and made to track the point source. The data was recorded. In the data analysis, the normalized cross-correlations between the reference antennas and the rest of the antennas were used to obtain the beam shape. Details of the experimental setup was as follows:

Table 1: Experimental details

Reference antennas	C01, C05
Sub-band	1280 MHz
LOI	1210 MHz
IF BW	32 MHz
LO4	70 MHz
BBW	8 MHz
LTA	4 sec
ALC	ON
Total grid points	11
Grid spacing	6'
Total grid extent	$\pm 30'$
Data length per point	2 min

For implementing the above procedure, we made a command file with the appropriate ONLINE commands for observing each grid point for 2 minutes. After setting up the DAS and starting the project, we ran the command file, part of which is shown here:

gts'ELE1'
sndsacsrc(1,1h)
trkelof(-30')
trksac(1,1h)
strtndasc
time 2m
stpndasc

The above few lines would observe the southern-most elevation grid point and acquire data for 2 minutes before moving on to the next command and hence represents one module of the command file. 'ELE1' is one of the dummy names created to recognise the grid point and hence ease the offline data analysis. The coordinates of ELE1, ELE2... were the same as the point source that we were observing, in this case, 3C48 ($S_{20cm} = 16.5$ Jy). It was important to remind the antennas to move to the point source before moving from one grid point to another. By running a command file made of many such modules, we acquired data for the one-dimensional grid of points. When the entire grid was covered, then the project was stopped and the data examined. A similar exercise was done for a grid in the azimuth.

For the third part of the experiment, we observed a coarser one-dimensional grid of points in elevation. The RF, IF, BB settings are given in following table: (The fractional

Table 2: Experimental details

Reference antennas	C01, C05
Sub-band	1060 MHz
LOI	1030 MHz
IF BW	32 MHz
LO4	66.4 MHz
BBW	8 MHz
LTA	4 sec
ALC	ON
Total grid points	7
Grid spacing	5'
Total grid extent	$\pm 25'$
Data length per point	2 min

numbers for LO4 is because we started this expt at the end of an observing session which used the above settings) The grid of seven points was repeatedly cycled through while tracking a strong point source, in this case, 3C286 ($S_{20cm} = 15$ Jy) through one observing run in order to catch the source at different elevations and study the variation in pointing offset. The cross-correlations with the reference antenna were used in the offline analysis. We also cycled through an azimuth grid of points, infrequently compared to the elevation grid to check for any azimuth offset dependence on elevation.

In the fourth part of the experiment, we scanned across a strong point source in the correlation mode and the relative sidelobe levels were examined. If the sidelobes were found to be asymmetric then the feed was rotated and the scan across the source taken again. The most optimum position of the feed was determined from the most symmetric sidelobe pattern obtained. More details of this part, the data and its analysis will be given in another report.

Using the subarray facility in ONLINE, we assigned the reference antennas, C01 and C05 to one subarray and the rest of the antennas (all available antennas were used in the experiment, however we concentrated mainly on the central square antennas) into another subarray, thus enabling independent control. C01 and C05 were used to track the source (3C48/3C286) and the rest of the antennas observed the grid points and the data were recorded.

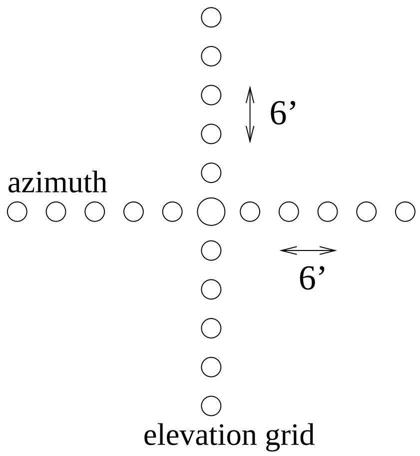

Figure 1: Grid of points observed along elevation and azimuth axes

3.1 Offline Analysis

The data obtained, thus, was analysed using locally developed software. *xtract* (author: Sanjay Bhatnagar) was used to time-average each of the 2m scans. No editing was effected before averaging. No channel-averaging was done. This data was written out in a *qdp* data file format. Since the normalized correlation coefficients would be in in voltage units for the antenna under consideration (the reference antenna give a constant signal which is correlated with the signal from the grid-observing antenna), these were squared using a routine written by one of us (NGK) to obtain the power pattern. The observed primary beam pattern for first three parts were fitted with a functional fort. We fitted a polynomial to these patterns in the software package *qdp* using a procedure written by one of us (APR). The procedure uses the polynomial-fitting routine within *qdp* after removing any pointing offset that the particular antenna may have. It invokes the *qdp* fitting routine and prompts the user to specify the pointing offset and the coefficients for the even indices of a polynomial to fit the beamshape i.e. coefficients for a constant, a quadratic, a biquadratic and a bicubic terms. The polynomial that fitted the azimuth beam well was:

$$P = 1 + a\,x^2 + b\,x^4 + c\,x^6 + d\,x^8 \tag{1}$$

where $x = x' - x_0$ where x' is the (distance from the peak in arcmin * freq in GHz) and x_0 is the pointing offset and a, b, c, d are the coefficients that we are interested in. The best model outputs are listed below. We also checked the goodness of gaussian fits to the beamshapes to examine the relative goodness of the eighth order polynomial and gaussian fits. A similar test was conducted using a sixth-order and 10th order polynomials. The eighth-order polynomial was found to give the best fit amongst these. The functional form for the gaussian that was fitted was:

$$G = \frac{1}{\sigma\,\sqrt{(2\Pi)}}\;a\;exp(-\frac{1}{2}(\frac{x-b}{\sigma})^2) \tag{2}$$

where a is the peak power, b is the pointing offset and σ is the dispersion. $HPBW = 2.354 * \sigma$.

For the third part of the experiment, the shift in the peak of the beam as the source elevation changes was examined by fitting a gaussian to each set of grid points about the source. This was effected in *qdp*. This procedure was done for a few antennas (C09, C14, C13, C04, C02, E05) and the offsets noted.

4 Results

The primary beam for both the elevation and azimuth grids are shown in Figures 2 to 5. Polynomial fits are superposed on the observed beam shape in Figs 2 and 3 whereas a gaussian fit is superposed on the observed beam in Figs 4 and 5.

4.1 The azimuth and elevation beams: symmetry

Examining Figs 4 and 5 which show the primary beams for the antennas C04, C09, C13, C14, it is fairly obvious that the azimuth beams are fairly symmetric compared to the elevation beams. For example, consider the elevation and azimuth beams for C09 in Figs 2 and 3. The azimuth beam is well-fitted by a gaussian and is symmetric while the elevation beam shows visible asymmetry. This is obvious in the case of the other antennas in Figs 4 and 5 also. Since the azimuth beam is symmetric down to $< 10\%$ points of the beam whereas the elevation beam displays asymmetry upto 30% points of the beam, the asymmetry in the latter could be due to the FPS position not being the optimum. Since the feeds are mounted on a turret which is rotated for observing different frequencies, if the FPS position is not correct, the elevation beam can display such asymmetries. The fourth part of the experiment was devised to obtain a more symmetric elevation beam.

4.2 The half power beam width (HPBW)

Gaussian fits to the power pattern (Figs 4, 5) yielded the following HPBW for the 1280 MHz sub-band.
Azimuth beamwidth was found to lie in the range 25.4' to 26.7'.
Elevation beamwidth was found to lie in the range 26.1' to 28.3'. Please note that all our experiments were done using only the 130 MHz polarization channel.

Since the elevation beams show some skewness, we consider only the HPBW obtained from the azimuth beams. The mean value is $\mathbf{26.1' \pm 0.7'}$. It should be scaled by the frequency from 1280 MHz to obtain the HPBW for the other frequencies and matches the values obtained using the total power scans (Vasant Kulkarni) across strong point sources (e.g. Virgo A, Cygnus A, Cas A).

If the GMRT antenna is a uniformly-illuminated circular aperture with diameter D, then its HPBW at a wavelength λ is given by $1.22\frac{\lambda}{D}$ for uniform illumination. This gives a value of $\sim 22'$ for the beam at 1280 MHz. However, the L-band feeds are tapered to obtain a compromise between the tapering efficiency and the spillover efficiency. To reduce the

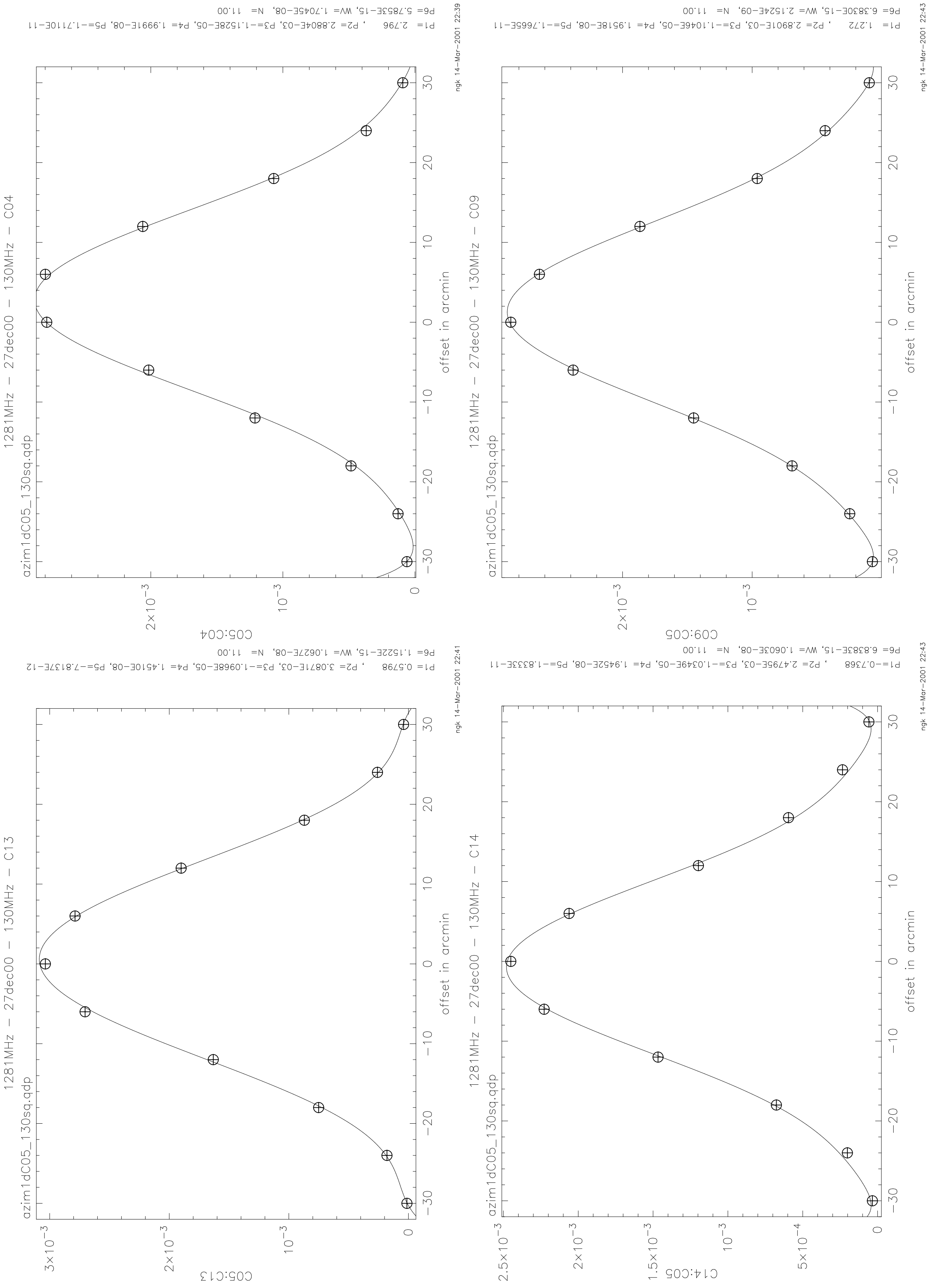

Figure 2: Eighth-order Polynomial fit to azimuth grid. The points are the observed data whereas the solid line shows the eighth order polynomial fit.

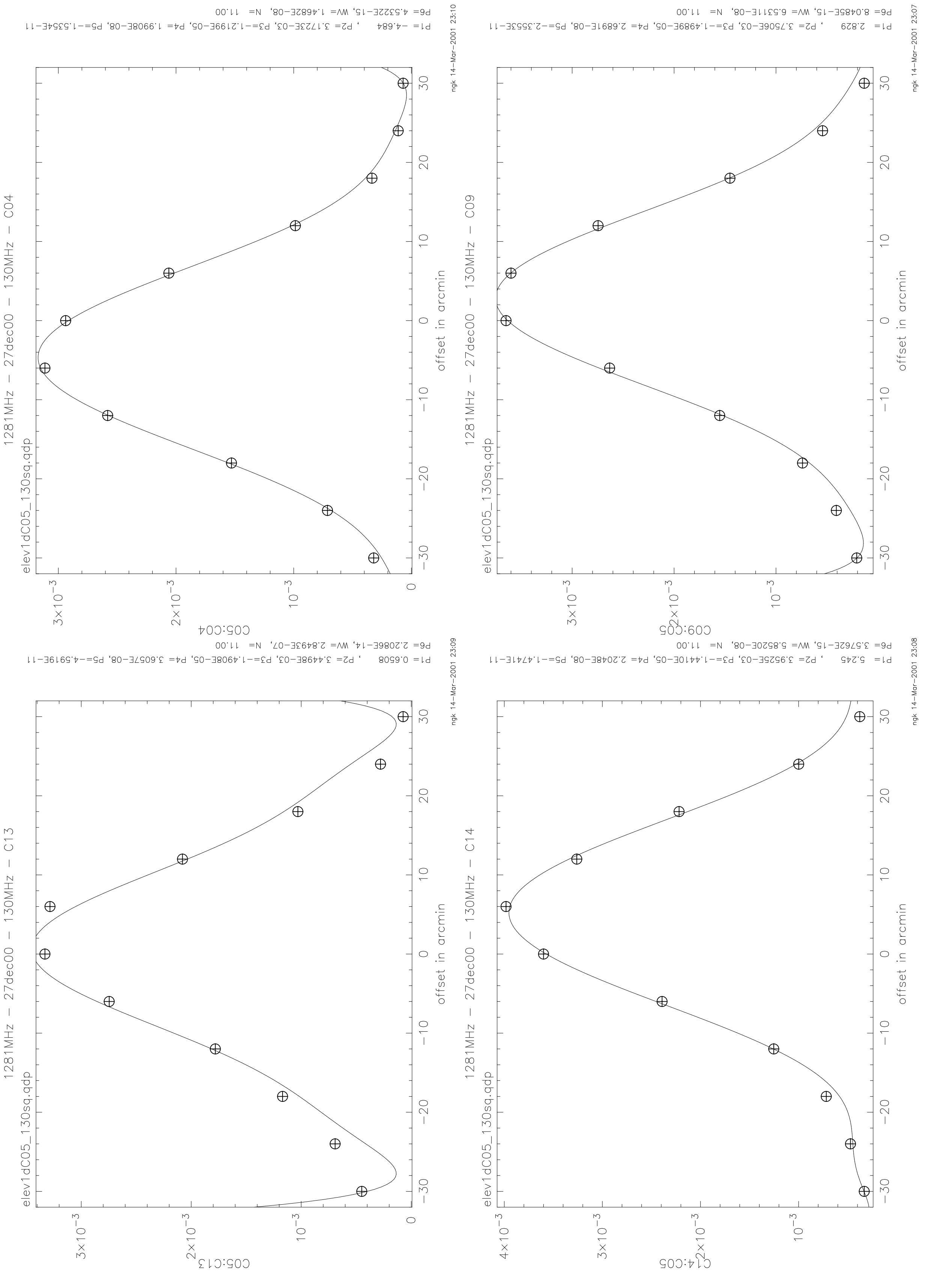

Figure 3: Polynomial fit to elevation grid. The points show the observed data whereas the solid line shows the eighth order polynomial fit.

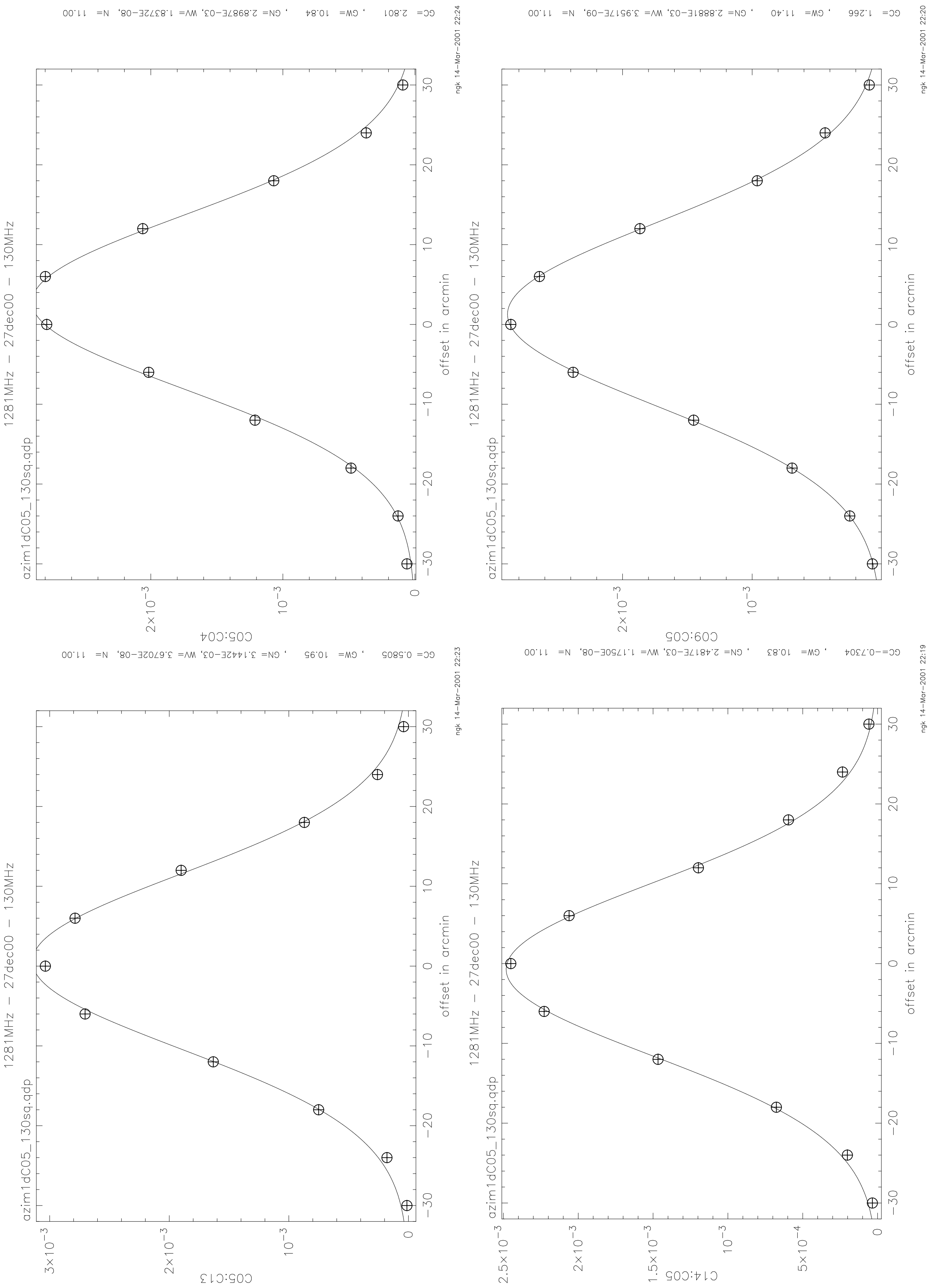

Figure 4: Gaussian fit to azimuth grid

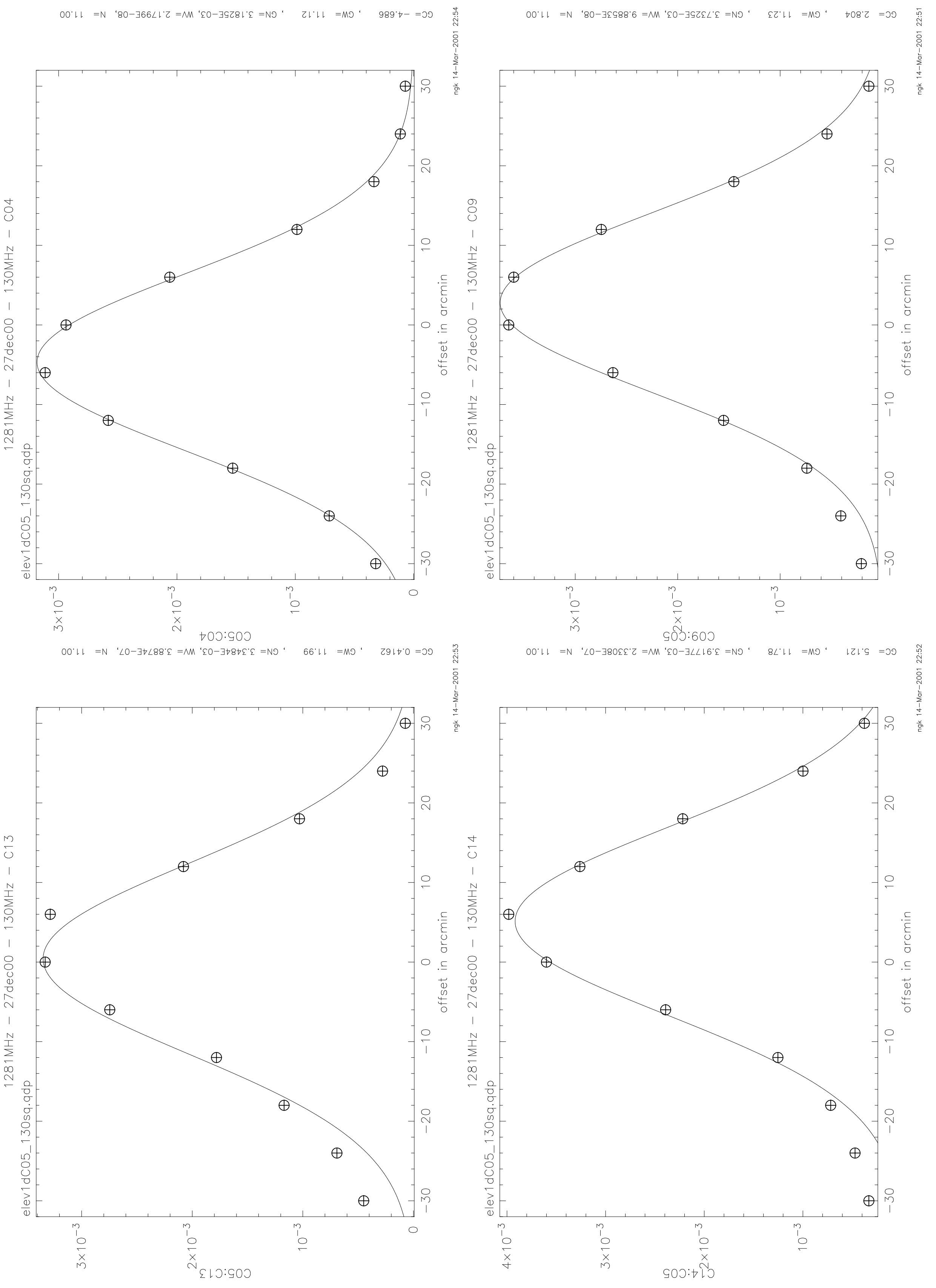

Figure 5: Gaussian fit to elevation grid

spillover, the aperture illumination is tapered, resulting in a wider beam, in this case a HPBW $\sim 26'$ at 1280 MHz.

Work to be done: It would be useful to repeat the one-dimensional grids along azimuth and elevation axes for the various sub-bands within L band and confirm the frequency scaling to the beamwidth and the present result.

4.3 Functional fits to the observed Beams required for primary beam gain correction

Below are tabulated the variance for the gaussian and polynomial fits to the azimuth beams for a few central square antennas. The variance for both an eighth-order and sixth-order polynomials are listed to show that the eighth-order gives the best fit to the beamshape.

Table 3: Comparing the variance of a gaussian, an eighth order polynomial and a sixth order polynomial fit to the primary beam.

Antenna	**Variance**		
	Gaussian	8th order polynomial	6th order Polynomial
C04	184	170	301
C09	40	22	140
C13	367	106	108
C14	118	106	192

The observed beams were approximated by eighth-order polynomials and the coefficients obtained. The eighth-polynomial functional form was fitted to the observed azimuth beams for a few antennas: C04, C09, C13, C14, S03 and W06 and the mean values for the coefficients obtained which are tabulated in table 4.3. A similar exercise was done for the elevation beams also and the mean coefficients listed in the Table 4.3 obtained from C04, C09, C14 and W06.

Table 4: Eighth order polynomial fit coefficients for the L band primary beam

Coefficient	**Azimuth beam**		**Elevation beam**
	Value	Uncertainty ($\sim 1\sigma$)	Value
a	-2.27961×10^{-3}	0.01×10^{-3}	-2.28152×10^{-3}
b	2.14611×10^{-6}	0.24×10^{-7}	2.21387×10^{-6}
c	-9.7929×10^{-10}	2.6×10^{-10}	-10.0982×10^{-10}
d	1.80153×10^{-13}	0.76×10^{-13}	1.78146×10^{-13}

The uncertainties are from the measured values. The peak-to-peak variation in the coefficients for the different antennas was noted and rms uncertainty obtained for the azimuth beam. Since we are not using the elevation beam; we have not calculated the error bars. Since these coefficients are normalized by the observed frequency, they need to be scaled to the appropriate frequency in the L band to get the desired polynomial fit to

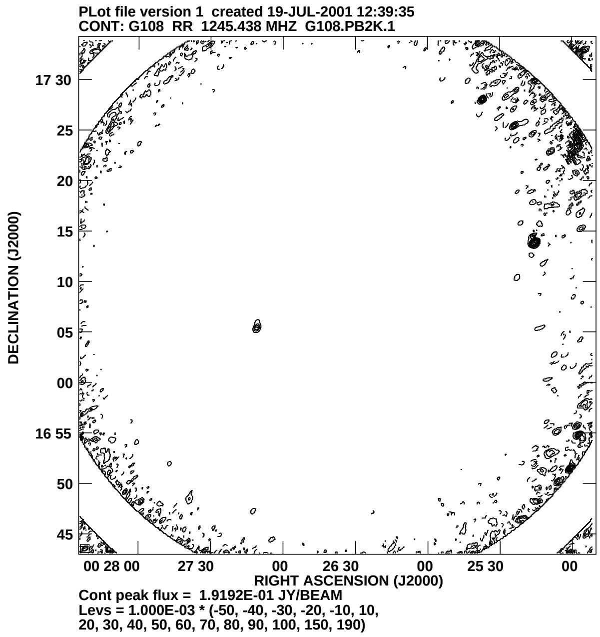

Figure 6: Primary beam gain correction on a field observed with GMRT at 1280 MHz.

the primary beam response. The x in Eq 3 is in terms of the frequency and the distance from the beam center in arcmin. The scaling is taken care of by the task PBCOR in AIPS which is discussed briefly in the next subsection. The correction should be effected to only 10% points of the main beam. Going to lower points is not advisable since the signal-to-noise ratio in those regions also degrades considerably and hence the image is not usable.

4.4 PBCOR in AIPS

The above coefficients are to be provided to the task PBCOR in AIPS (Astronomical Image Processing System) for implementing the primary beam correction to the data in the image plane. We entered the coefficients in the DPARM adverbs in PBCOR and applied it to an image at 1280 MHz. The result is shown in Fig 6.

The field shown in Fig 6 is clean with only a couple of sources visible: one to the east of the phase center and another north-west of the phase centre which is almost buried in the beam edge noise. The edges of the beam are noisy due to the poor signal-to-noise ratio. The noise which is seen in the four corners of the image is due to the polynomial fit rising at the beam-edges much below the 5% points. Since this is not the region of the beam that we are interested in, it can be ignored except for the aesthetically-compromised image! We measured the peak brightness of three point sources visible in our image and compared the flux to that found from the NVSS image downloaded from the net. This was done to check the functioning of the polynomial fit. The uncorrected and corrected flux densities of the sources are also tabulated.

From Table 4.4, the increase in the flux densities effected by the primary beam cor-

Table 5: Primary beam gain correction

α_{2000} hh mm ss	δ_{2000} $^\circ$ $'$ $''$	S1(1280 MHz) Before PBCOR	After PBCOR	S2(1420 MHz) NVSS	S1 (After PBCOR) /S2
00 25 16	17 13 51	42 mJy	214 mJy	268 mJy	0.80
00 27 11	17 05 30	54 mJy	70 mJy	92 mJy	0.76
00 25 37	17 28 01	6 mJy	68 mJy	188 mJy	0.36

rection is evident in columns 3 and 4. The NVSS values are listed in column 5 whereas column 6 gives the ratio of the gain-corrected flux densities from our 1280 MHz map and the NVSS 1420 MHz map. The first and second sources are clearly visible in Fig 6 whereas the third source is buried in the noise and not clearly discernible here. So considering only the first two sources, the flux density seems to have been properly gain corrected since the ratio is constant at ~ 0.8. The lower 1280 MHz flux densities are most probably due to an amplitude scale error. The last point is $\sim 1\sigma$ in the uncorrected map and hence should not be overemphasized. Hence to first level, the primary beam correction seems to be working.

Work to be done: Scaling the primary beam coefficients to other frequencies has to be checked out. It would be useful to use the above coefficients in AIPS and correct the other sub-band frequencies and compare with published maps like the NVSS.

4.5 Variation in Pointing offsets as a function of Source Elevation

The offsets obtained by fitting a gaussian to each grid was plotted against the elevation of the source as shown in Fig 7 & 8. We find that the elevation pointing offsets vary within $4'$ for five of the six antennas that we studied. The figures (Fig 7) show these results clearly. The errors on the data when C01 was used as the reference antenna are somewhat lower than those for C05 as reference antenna and a slow variation in the elevation pointing offset as the elevation of the source changes is evident in the data. Unfortunately we did not have data between hour angles -1h and 2h ie near the transit of the source - however the trend is clearly seen. The jump in some of the offsets after transit ie after crossing elevation of 90° is due to an understood servo problem which is being presently addressed by the engineers. The azimuth data (Fig 8) has been given for comparison and as expected there is little change in the offsets with elevation.

Work to be done: 1) This experiment needs to be repeated a couple of times to try and get a functional form for the variation in pointing as a function of elevation. 2) Software for the data analysis needs to be developed.

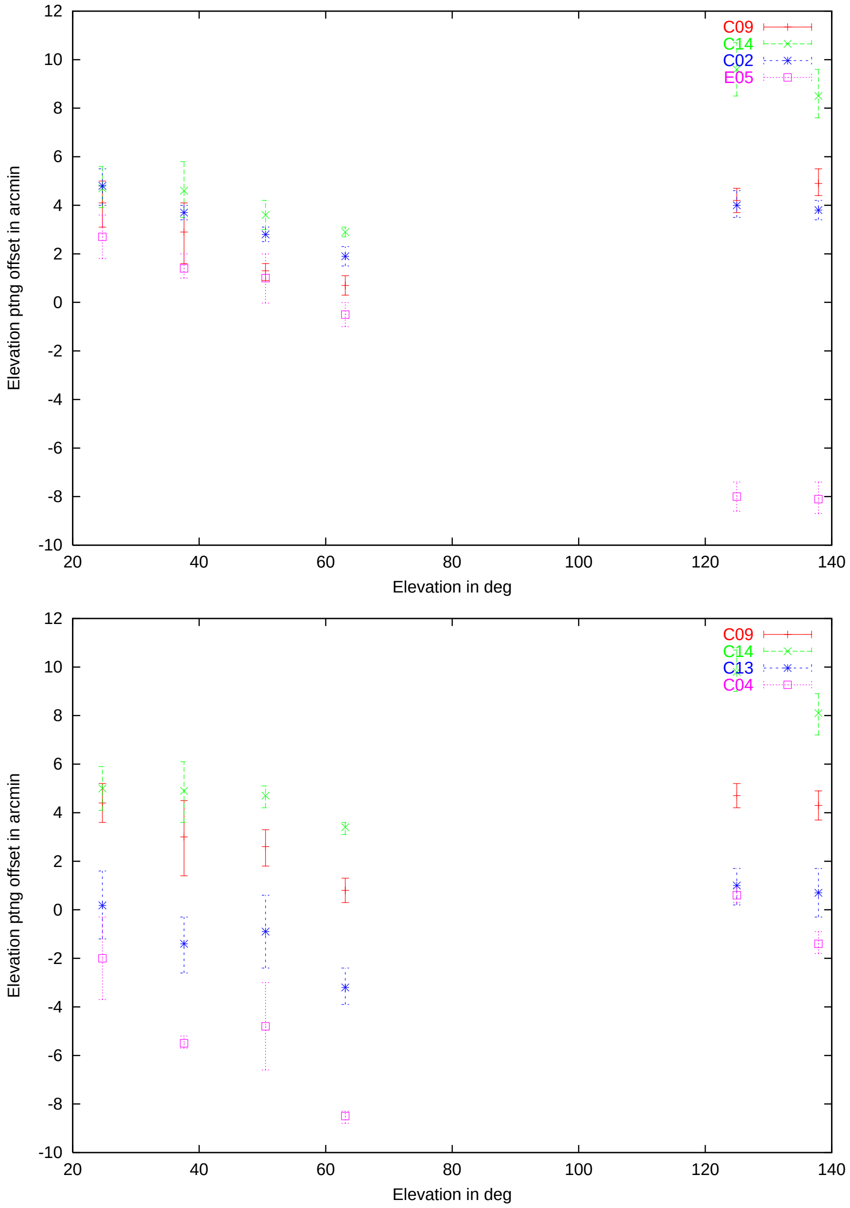

Figure 7: Variation in pointing offsets as a function of elevation. The elevation has been taken to run from 0 to 180° for convenience. For any $x > 90°$ in the figure, $elevation = (x - 90)°$. The top panel shows the elevation offsets for four antennas C09,C14,C02,E05 where C01 has been used as the reference antenna. The bottom panel shows the same for C09,C14,C13,C04 using C05 has the reference antenna. A slow variation in pointing with elevation is observed.

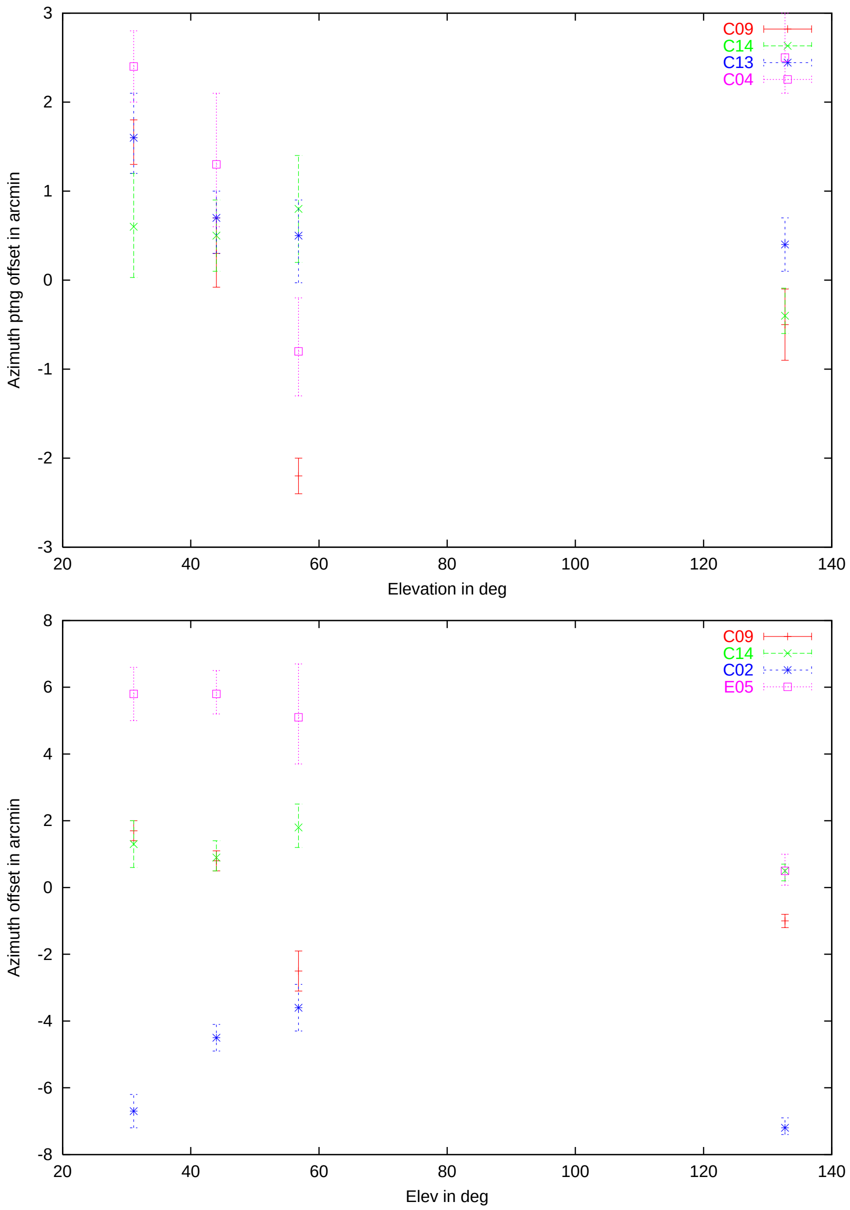

Figure 8: Figure shows the azimuth pointing offsets as a function of elevation of the source for C09,C14,C13,C04 using C05 as the reference antenna. Note that the variation for most antennas is $< 2'$. The lower panel is for C01 as reference and includes two other antennas

5 Summary

The entire experiment was divided into four parts to study four aspects related to the L band beam. The 130 MHz polarization channel was used. The first part concerned the study of the beamshape in both the altitude and azimuth directions and the half power beamwidth at 1280 MHz was obtained. For this we obtained a one-dimensional cut in elevation and azimuth by observing a grid of points about a strong point source. While the azimuth beam is fairly symmetric, the elevation beam was found to be skewed. The half power beamwidth at 1280 MHz was found to be $26.1' \pm 0.7'$. The second part was to use this data and find the best polynomial fit to the beamshape. This is required for correcting the GMRT data for the primary beam gain variation. An eight-order polynomial fit was found to fit the azimuth beam well and the mean coefficient values are presented here. In the third part to study the variation in elevation pointing offsets with source elevation, we tracked a strong point source through a run and noted down the offsets. The offsets do not vary significantly, but they do show a systematic variation of $\leq 4'$. Lastly, to obtain an optimum position for the FPS, the fourth part of the experiment by rotating the feed turret to obtain a more-symmetric elevation beam was devised. The data and discussion can be found in another report.

NGK thanks Sanjay Bhatnagar and G. Shankar for useful discussions. Presently, more data and information has been gathered following some more system tests regarding the L band beamshape and the optimum position of the feed positioning system. These results will be presented in a separate report.

6 References

Shankar G., SERC School lecture series... chapter 3.